ADVANCED OPTICAL MATERIALS

Supporting Information

for *Adv. Optical Mater.*, DOI 10.1002/adom.202202497

Superradiance Emission and Its Thermal Decoherence in Lead Halide Perovskites Superlattices

Hamid Pashaei Adl, Setatira Gorji, Guillermo Muñoz-Matutano, Andrés F. Gualdrón-Reyes, Isaac Suárez, Vladimir S. Chirvony, Iván Mora-Seró and Juan P. Martínez-Pastor**

Supporting Information:

Superradiance emission and its thermal decoherence in Lead Halide Perovskites Superlattices

*Hamid Pashaei Adl**, *Setatira Gorji*, *Guillermo Muñoz-Matutano*, *Andrés F. Gualdrón-Reyes*, *Isaac Suárez*, *Vladimir S. Chirvony*, *Iván Mora-Seró*, and *Juan P. Martínez-Pastor**

Dr. H. Pashaei Adl, Ms. S. Gorji, Dr. G. Muñoz-Matutano, Dr. I. Suárez, Dr. V. S. Chirvony, and Prof. J. P. Martínez-Pastor
Instituto de Ciencia de Materiales (ICMUV), Universidad de Valencia, C/ Catedrático José Beltrán, 2, E-46980 Paterna, Spain.
E-mail: Hamid.pashaeiadl@uv.es; Juan.Mtnez.Pastor@uv.es
Dr. I. Suárez
Departamento de Ingeniería Electrónica, Escuela Técnica Superior de Ingeniería, Universidad de Valencia, Avenida de la Universidad s/n, 46100 Burjassot, Spain.
Dr. A. F. Gualdrón-Reyes, Prof. I. Mora-Seró
Institute of Advanced Materials (INAM), Universitat Jaume I, Avenida de Vicent Sos Baynat, s/n, 12071, Castelló de la Plana, Spain.
Dr. A. F. Gualdrón-Reyes
Facultad de Ciencias Instituto de Ciencias Qumicas, Isla Teja, Universidad Austral de Chile, Valdivia 5090000,Chile.

Below, several figures are shown as complementary results to support our work. Most of the information about these results are given in the figure caption

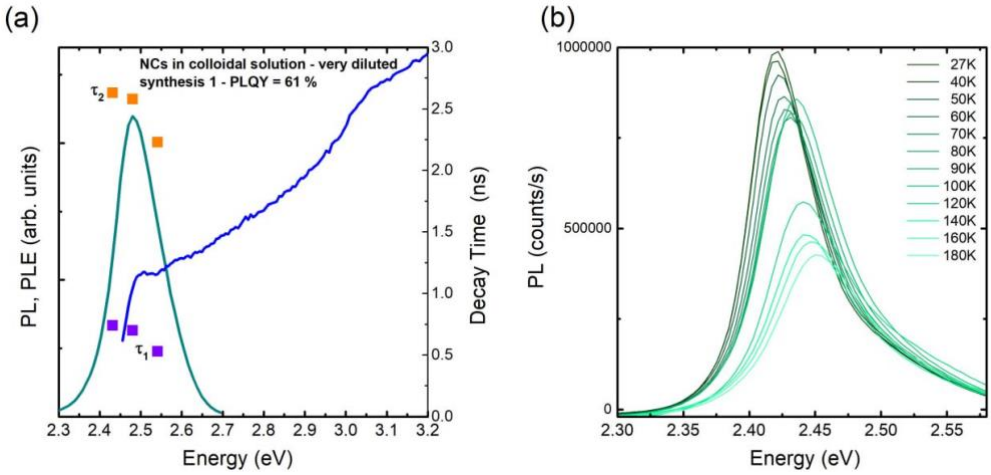

Figure S1. PL and PLE spectra measured in a colloidal solution containing NCs used for superlattices type A used in the present work (b) PL spectra for different temperatures measured with standard PL setup in a film prepared by dipping the substrate in the same solution used for the SL fabrication.

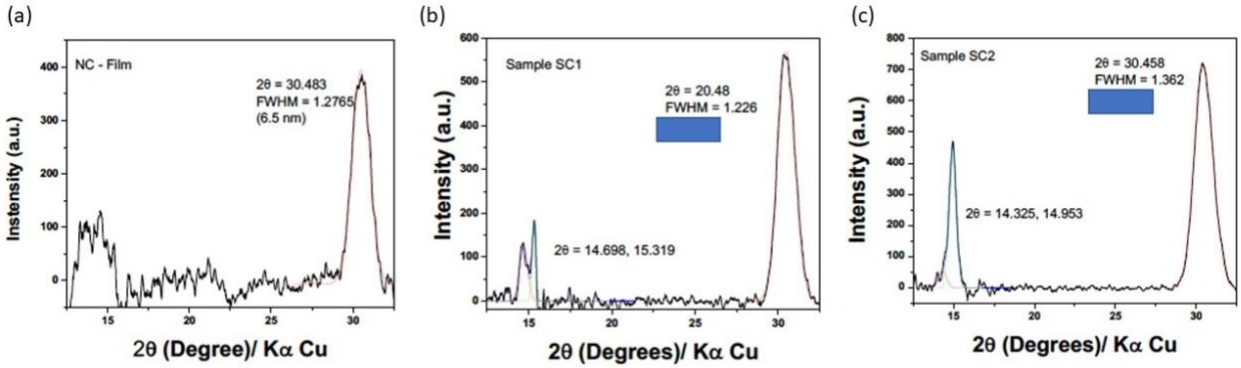

Figure S2. θ–2θ X-Ray Diffratograms in the region 10-35º made in the film (a) and two different samples with supercristals (b-c) prepared under similar conditions. The θ - 2θ X-Ray Diffraction of type A SLs is presented in Figure S2 in comparison with a uniform film prepared by dipping into the same concentrated solution used for the fabrication of the SLs. In the film, we recognize the peak at around 2θ = 30.5° (Figure S2 (a)), which is a clear signature of the $CsPbB_3$ material (cubic or with tetragonal/orthorhombic deformation) and some contributions at around 15° and 21-22°. However, in the case of SLs, we clearly observed a preferential orientation of the nanocubes, because only observed diffractions of (001), in the region of 2θ around 15°, and (002) at 2θ = 30.5°. In the two available samples for type A SLs, we observed a double peak structure at 2θ = 14.7-15.3° for SC1 and 2θ = 14.33-14.95° for SC2, as shown in figures S2 (b) and (c), respectively.

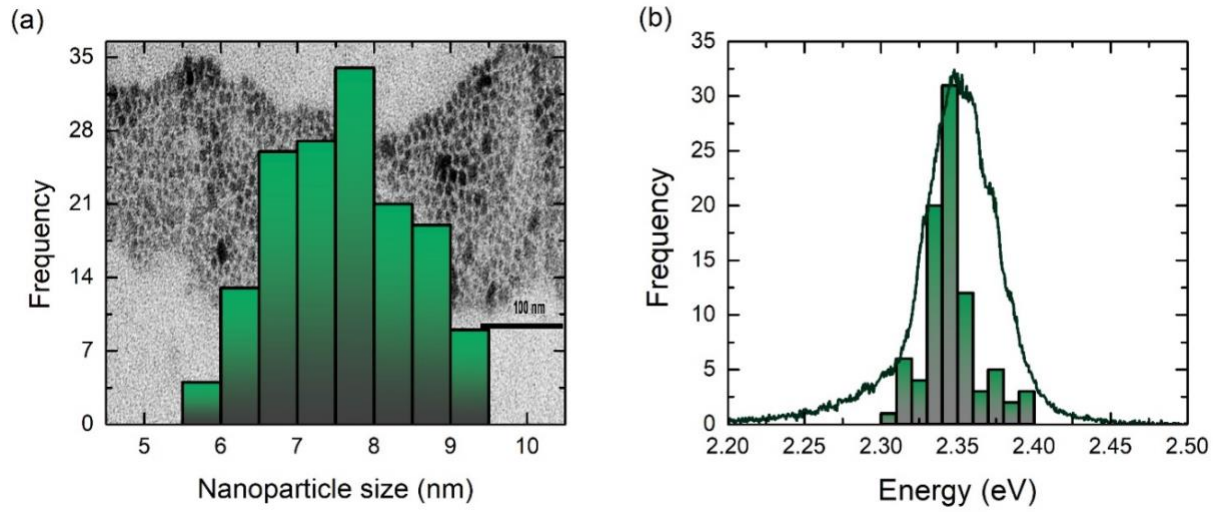

Figure S3. (a) Histogram of NC sizes obtained from low resolution TEM images (the real values for the edge size can be slightly larger than those shown here, because the TEM was taken several weeks later and precipitation over time can introduce a reduction of the average size of NCs in solution), (b) Statistics (dark blue bars) obtained for the micro-PL peak energies in around 100 $CsPbBr_3$ single NCs as compared to the micro-PL spectrum (black curve) of the corresponding high-density sample, all measured at 4 K.

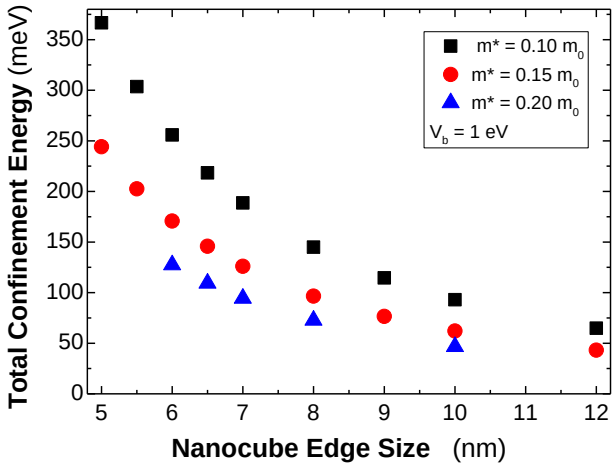

Figure S4. Estimated total (electron + hole) confinement energy in 3D square quantum wells (a cubic NC) on the basis of a 1D square quantum well (transcendental equation below, using effective masses equal for electrons and holes in the range 0.1-0.2 m_0, and a potential barrier height of 1 eV) (*).

(*) Confinement energy in NCs and Superlattices

For a 3D square quantum well, the total confinement energy (the sum of those for electrons and holes) would be approximately estimated by multiplying by 6 (assuming here the same effective mass for electrons and holes in the $CsPbBr_3$ perovskite) the value obtained using the transcendental equation for a single 1D quantum well:

$$\cos(k_w L) - \frac{1}{2}\left[-\tilde{\xi} + \frac{1}{\tilde{\xi}}\right]\sin(k_w L) = 0 \qquad \xi \to i\tilde{\xi};\ \ \tilde{\xi} = \frac{k_b}{k_w}$$

$$k_b = 0.162\sqrt{V_b - \varepsilon}\ \ (nm^{-1}) \qquad k_w = 0.162\sqrt{m^*\varepsilon}\quad (nm^{-1})$$

For the barrier we assumed directly the electron mass in vacuum. In the estimation of the carrier confinement energy the assumed potential barrier defined by the ligands (oleic/oleylamine) would not influence provided it is higher than 1 eV.

Figure S4 shows estimated values of the total confinement energy of carriers for several edge lengths (L) of the NCs and the most probable effective masses (usually reported from calculations in the range 0.1 – 0.2 m_0). From these calculated values we can estimate a variation dE_c/dL of around 30 meV/nm for a NC size around 8 nm using m* = 0.15 m_0. The slope would be higher (lower) for m* = 0.1 m_0 (0.20 m_0) and decreases by increasing the edge length of the NC.

We can also estimate the shift and miniband width in the case of assembled NCs in the order of 3 meV (for overall shift of the optical transition and total miniband width for electrons and holes) for a SL formed with NCs of 7 nm edge size and assuming a barrier thickness of 1 nm. Larger barriers (in the case of OA/OAM can be in the order of 2 nm) will reduce (exponentially) below that energy. The estimate is based on the solution of the following transcendental equation by taking into account a Bloch-like wavefunction:

$$\cos(qd) = \cos(k_w L)\cosh(k_b h) - \frac{1}{2}\left[-\tilde{\xi} + \frac{1}{\tilde{\xi}}\right]\sin(k_w L)\sinh(k_b h)$$

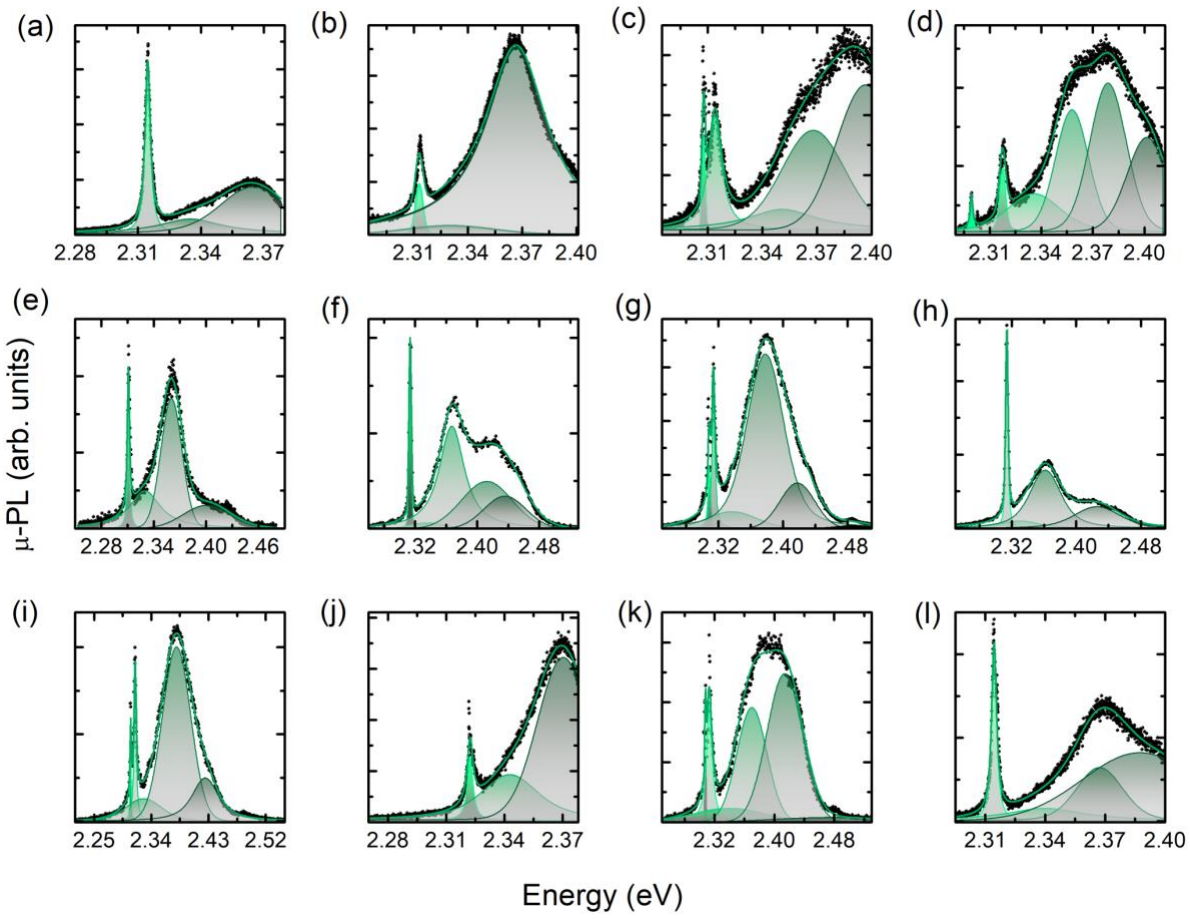

Figure S5. μ-PL spectra measured at 4 K in most of the type B SLs using continuous wave excitation at 405 nm.

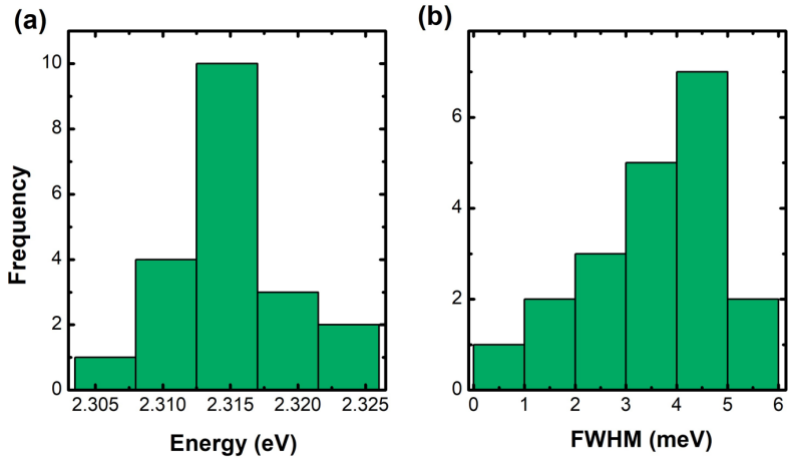

Figure S6. The histogram of (a) peak energies and (b) FWHM extracted from Lorentzian fits of LEC narrow lines in μ-PL spectra of 20 type B $CsPbBr_3$ SLs prepared with NCs shown in Figure S3.

Power (nW)	$FWHM_{P1}$ (meV)	$FWHM_{P2}$ (meV)	$FWHM_{P3}$ (meV)	$(FWHM_{P1} + FWHM_{P2}) = FWHM_{total}$ (meV)
28	1.51±0.14	3.76±0.13	53.45±0.37	5.27
72	2.32±0.21	3.81±0.16	55.41±0.40	6.13
112	2.01±0.18	4.16±0.18	57.54±0.44	6.17
168	2.53±0.22	4.06±0.19	59.56±0.47	6.59
280	3.69±0.30	4.35±0.24	61.57±0.47	8.04
464	4.20±0.37	5.14±0.31	62.28±0.48	9.34
732	5.41±0.47	5.64±0.48	63.48±0.48	11.05
1012	6.68±0.37	5.97±0.38	63.57±0.43	12.65
1680	7.50±0.44	6.83±0.45	63.76±0.40	14.33
3320	———	14.52±0.32	64.05±0.50	14.52
6000	———	15.60±0.40	65.23±0.52	15.60

Table S1: Spectral broadening of LEC and HEC emission lines in type B $CsPbBr_3$ SLs by increasing the excitation power.

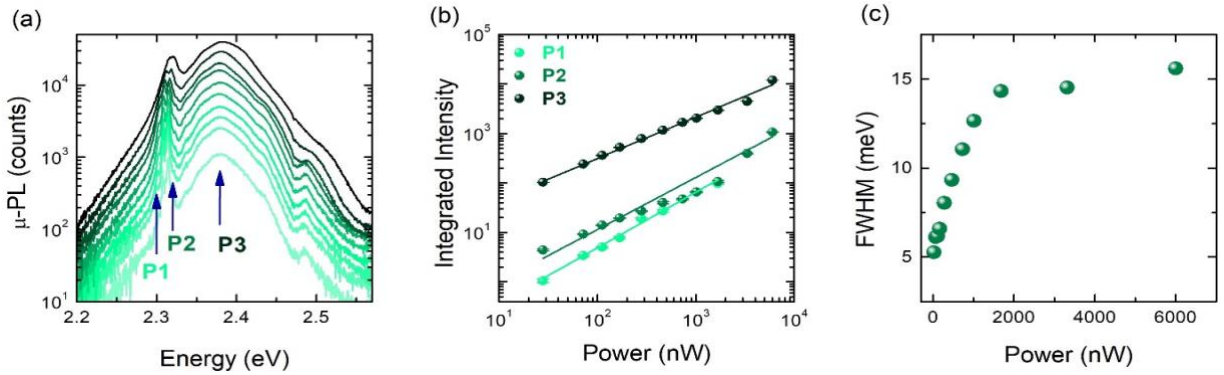

Figure S7. (a) Color-coded power-dependent PL emission of $CsPbBr_3$ type B SLs by increasing pulsed excitation power from 25 nW (faded green) to 6μW (black), (b) PL intensity integrated over the spectral emission range of LEC (SR intensity, cyan and light green spheres), with slopes $m_{P1} = 1.13 \pm 0.04$, $m_{P2} = 1.05 \pm 0.05$, and HEC with slope $m_{P3} = 0.84 \pm 0.03$ (HEC intensity, olive green spheres) in a log-log plot. (c) Total LEC emissions broadening as a function of excitation power at 4K (values from table S1).

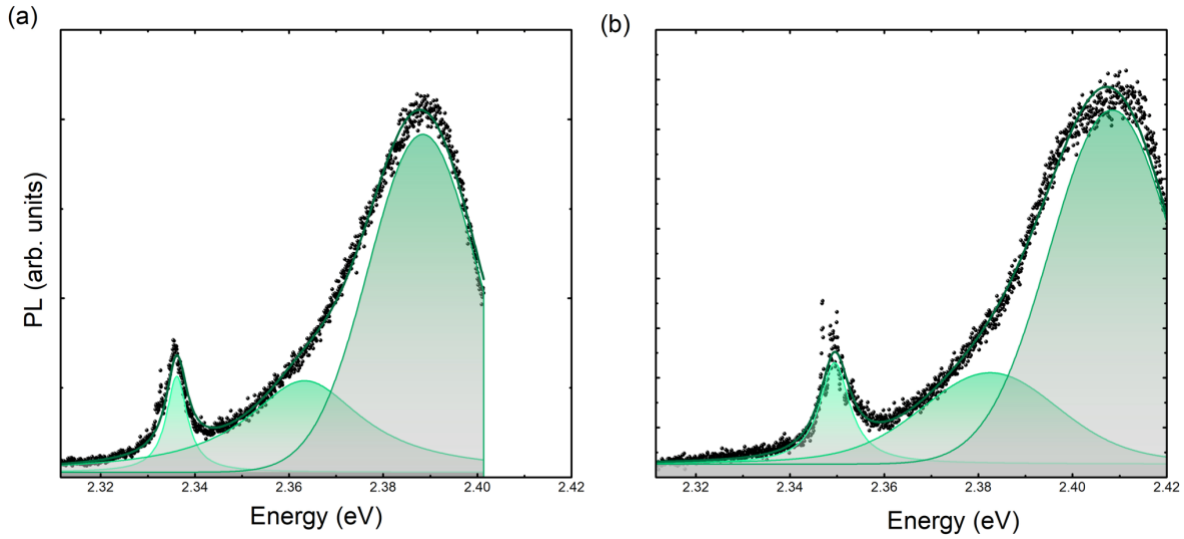

Figure S8. µ-PL spectra at 4 K in two type B SLs exhibiting LEC peak out of the statistics above (Figures S5-S6) and best fitting to Lorenzian (LEC) shape and two HEC emission bands.

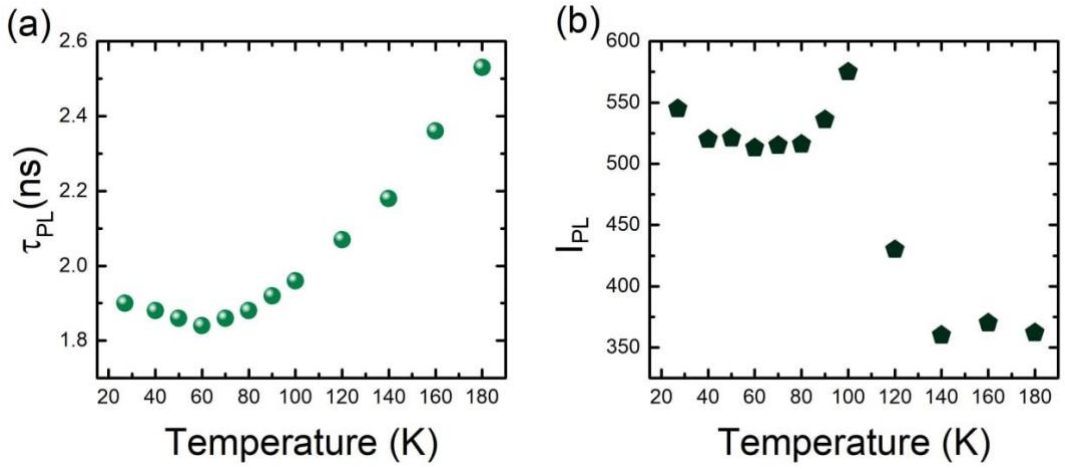

Figure S9. Variation with temperature of decay time (a) and integrated PL intensity (b) (from spectra in Figure S1b) measured in thin films prepared with the colloidal NCs in Figure S1a (those used for the self-assembled growth of type A SLs). From the PL intensity dependence, we can say that exciton recombination is mostly radiative until around 100 K.

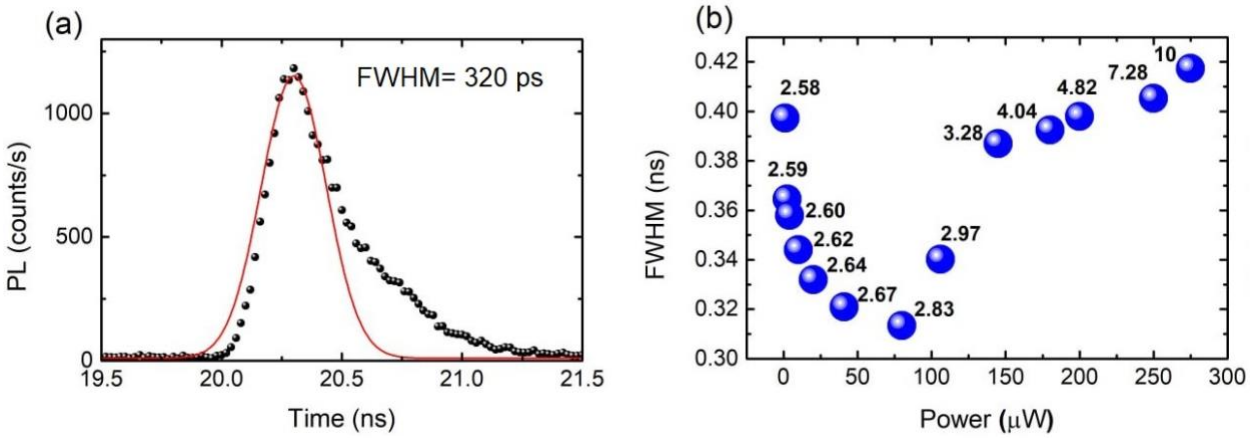

Figure S10. Time response in our experimental setup using either a doubled fs-pulsed Ti:sapphire laser at 405 nm (a) or a ps-pulsed laser diode at 450 nm at different powers (b).

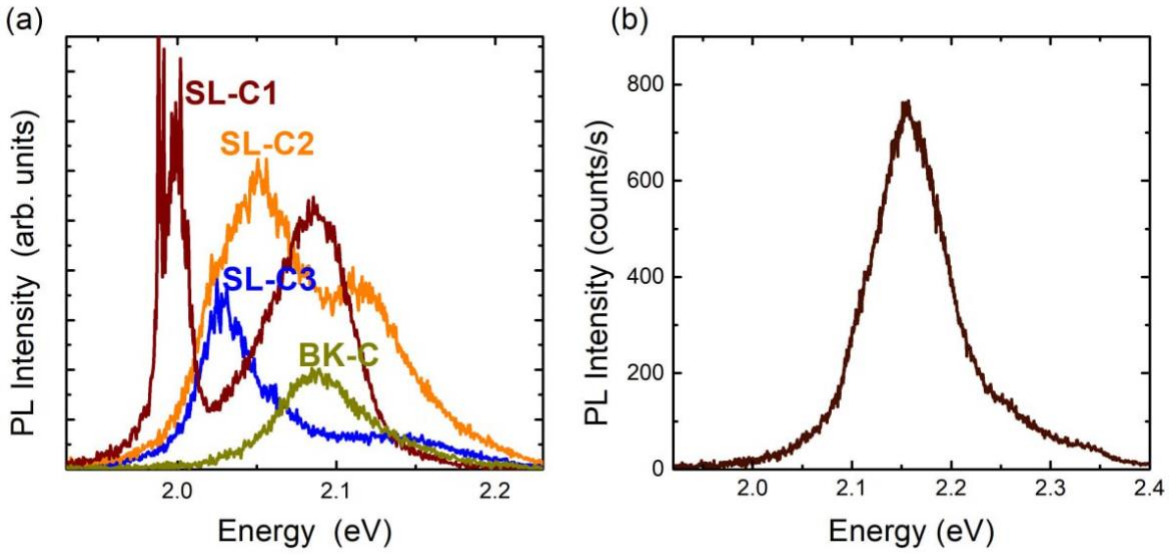

Figure S11. μ-PL spectra measured at 4 K in three different type C SLs (with alloyed $CsPbBrI_2$ NCs) and background in between SLs (a), as indicated in the plot, and that measured in a thin film prepared with the same NCs (b).

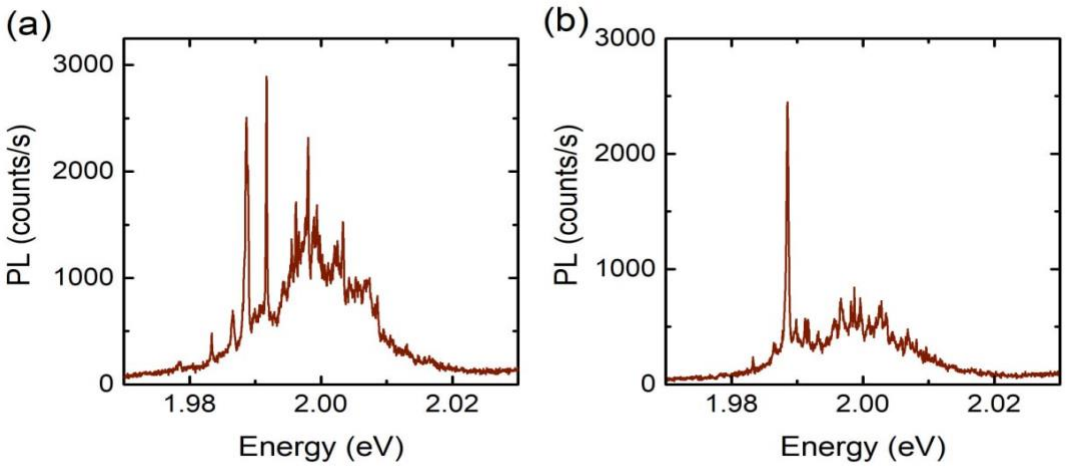

Figure S12. Detail of the μ-PL spectra in the region of the LEC emission for two type C SLs at 4 K (very low power and continuous wave laser at 405 nm) exhibiting very narrow lines that are typically observed over the low energy side of the LEC emission band.

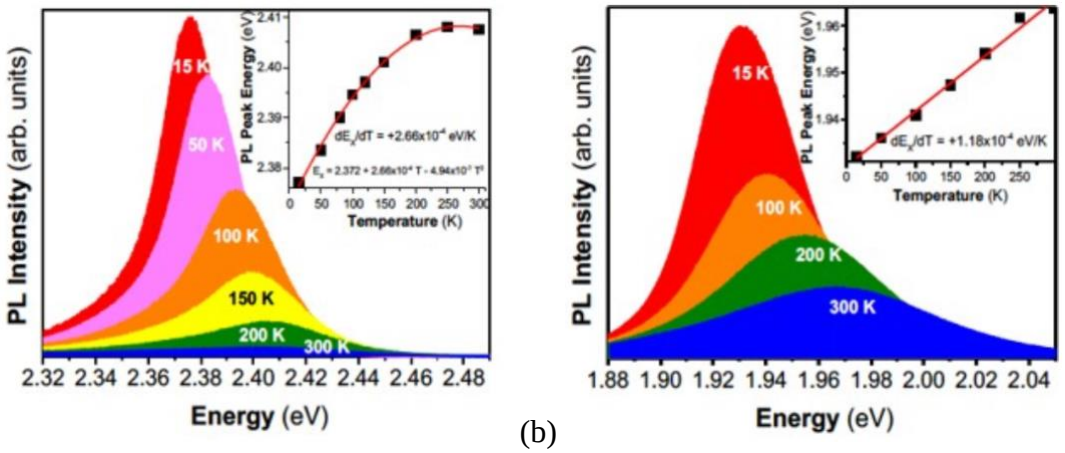

(a) (b)

Figure S13. Ensemble-PL evolution with temperature in thick layers of uncoupled NCs of $CsPbBr_3$ (a) and $CsPbBr_{1.2}I_{1.8}$ (b). The PL emission of NCs increases in energy in the order of 9 (20) meV at 50 (100) K for $CsPbBr_3$ NCs and half of these values for alloyed NCs.

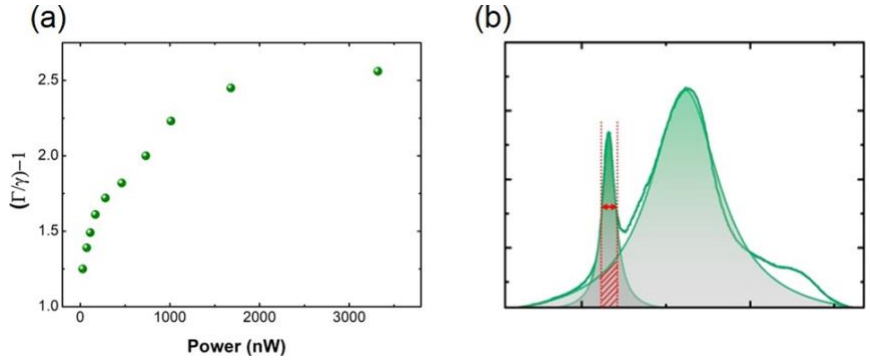

Figure S14. (a) Normalized LEC emission (SR) enhancement factor ($\frac{\Gamma}{\gamma} - 1$), as a function of the excitation power, (b) Graphical representation of the integration range of LEC and HEC emissions for calculating the SR enhancement factor. The power-dependent broadening (a factor 3 up to 2 µW) has a certain effect on the LEC emission enhancement factor, as determined by our proposed method, hence low excitation powers are used for all investigated type B SLs and used for figure 6c in the body of the manuscript.

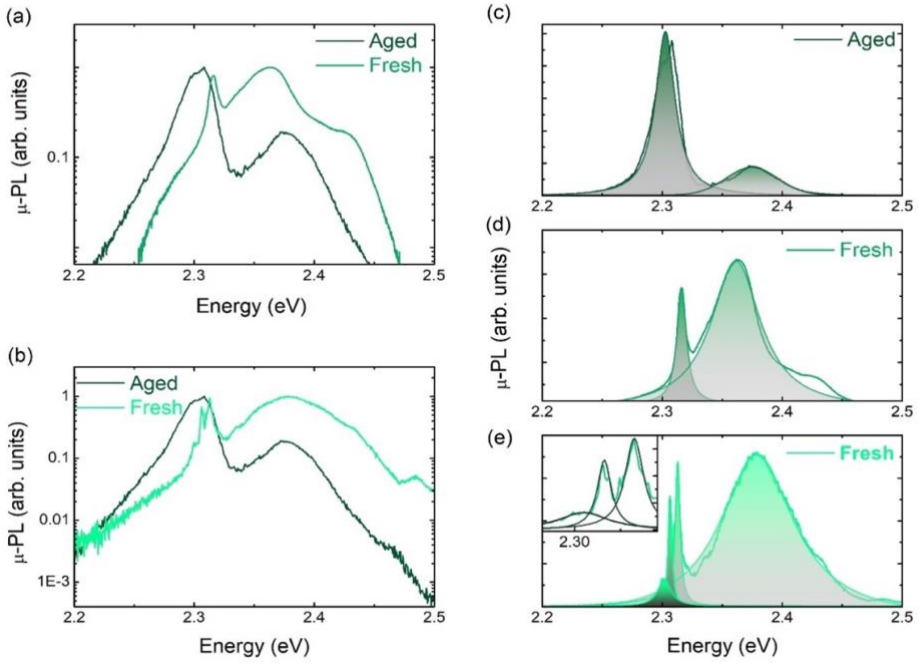

Figure S15. (a) μ-PL spectra in logarithmic scale of an aged type B SL (dark green) measured under an excitation power of 6 µW and a fresh type B SL exhibiting a single SR emission (light green) under the same excitation power. (b) Idem for a different fresh type B SL exhibiting three SR emission lines measured under low excitation power (50 nW). (c)-(e) The same µ-PL spectra corresponding to these SLs, aged (c) and fresh ones (d)-(e) in linear scale; the zoom in (e) is a zoom of the LEC zone with the three SR lines. All measurements were performed at 4K

under continuous wave excitation at 405 nm. It is worth noting how the estimation of the enhancement factor as proposed in Figure S14(b) does not give a reasonable value in the case of the aged SL, because the low energy line (centered at 2.30 eV) is well below the HEC at around 2.375 eV and both lines have similar linewidths.

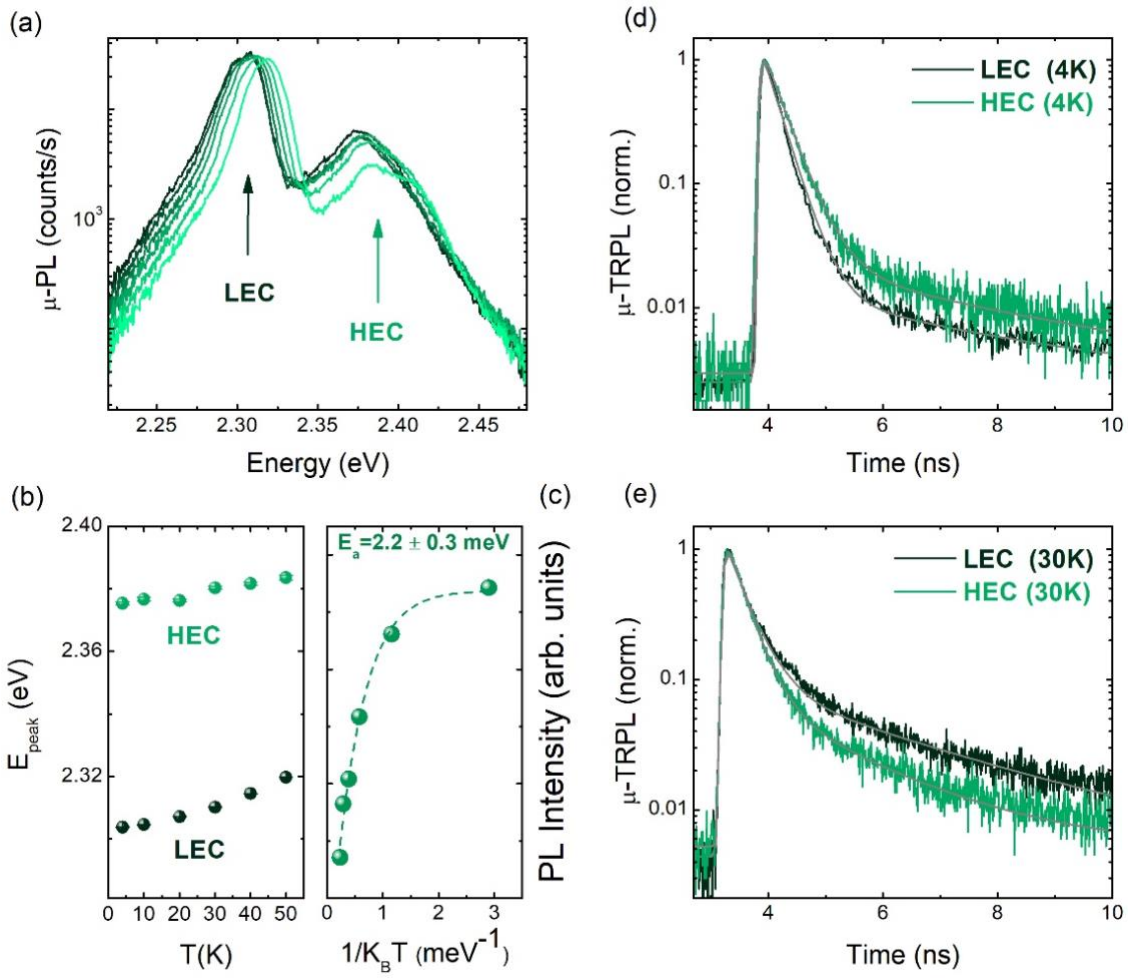

Figure S16. (a) μ-PL spectra of an aged $CsPbBr_3$ SL (type B) as a function of temperature ranging between 4- 50K. (b) Variation of the LEC and HEC peak energies (obtained from fittings of spectra in (a)) as a function of temperature (c) Arrhenius plot of the LEC emission for the aged $CsPbBr_3$ SL, fitted with an activation energy $E_a = 2.2$ meV. (d), (e) μ-TRPL spectra measured in the same aged $CsPbBr_3$ SL at 4K and 30K, respectively. Dark (light) green lines correspond to μ-PL transients measured at LEC (HEC) peak energy, which were fitted with τ_1(4 K) = 248 ps and τ_1(30 K) = 364 ps (τ_1(4 K) = 398 ps, τ_1(30 K) = 441 ps).